$\mathcal{R}$esearch in
$\mathcal{A}$stronomy and
$\mathcal{A}$strophysics

Flux density measurements for 32 pulsars in the 20 cm observing band

Yan-Wei Xie[1,2], Jing-Bo Wang[3,4], George Hobbs[5,2], Jane Kaczmarek[5], Di Li[2,6], Jie Zhang[1,7], Shi Dai[5], Andrew Cameron[5], Lei Zhang[2,5], Chen-Chen Miao[2,6], Mao Yuan[2,6], Shen Wang[2,6,8], Song-Bo Zhang[9,5], Heng Xu[10,11,2], Ren-Xin Xu[10,11]

[1] School of Physics and Space Science, China West Normal University, Nanchong 637002, China
[2] National Astronomical Observatories, Chinese Academy of Sciences, Beijing 100101, China
[3] Xinjiang Astronomical Observatory, Chinese Academy of Sciences, Urumqi 830011, China; *wangjingbo@xao.ac.cn*
[4] Key Laboratory of Radio Astronomy, Chinese Academy of Sciences, Urumqi 830011, China
[5] CSIRO Astronomy and Space Science, PO Box 76, Epping, NSW 1710, Australia
[6] CAS Key Laboratory of FAST, National Astronomical Observatories, Chinese Academy of Sciences, Beijing 100101, China
[7] College of Physics and Electronic Engineering, Qilu Normal University, Jinan 250014, China
[8] Astronomy Department, Cornell University, Ithaca, NY 14853, USA
[9] Purple Mountain Observatory, Chinese Academy of Sciences, Nanjing 210008, China
[10] Kavli Institute for Astronomy and Astrophysics, Peking University, Beijing 100871, China
[11] Department of Astronomy, School of Physics, Peking University, Beijing 100871, China

Abstract Flux densities are fundamental observational parameters that describe a pulsar. In the current pulsar catalogue, 27% of the listed radio pulsars have no flux density measurement in the 20 cm observing band. Here, we present the first such measurements for 32 pulsars observed employing the Parkes radio telescope. We have used both archival and new observations to make these measurements. Various schemes exist for measuring flux densities and we show how the measured flux densities vary between these methods and how the presence of radio-frequency interference will bias the flux density measurements.

Key words: methods: data analysis — pulsars: general

1 INTRODUCTION

Measurement of a pulsar's flux density in one or more observing bands reveals information on the pulsar emission process (for instance, through measurements of the spectral index of the emission; e.g., Kijak et al. 2017) as well as providing a means to probe the interstellar medium (e.g., Keith et al. 2013; Levin et al. 2016; Kerr et al. 2018). As almost all the major radio observatories carry out observations in the 20 cm observing band, knowledge of pulsar flux densities in this band is essential. Such information is used to predict how many pulsars a new survey may discover, to explain why some pulsars are not detected in a particular observation and to select key, bright pulsars to observe for commissioning or calibration observations.

The Australia Telescope National Facility (ATNF) Pulsar Catalogue (Manchester et al. 2005) houses a repository for pulsar observational parameters. Out of the 2659 radio pulsars in the catalogue (we have used the most up-to-date version, 1.59), 704 do not have a flux density determination in the 20 cm observing band. Some of these are surprising; for instance, PSR J1506−5158 was discovered in 1978 and modern-day instrumentation can easily obtain high signal-to-noise ratio (S/N) profiles for this pulsar with minimal integration time. We have, therefore, begun a project with the goal of completing the parameterisation of the pulsars in the catalogue and we have started with the missing flux density measurements. We note that even though flux densities are fundamental properties of a pulsar, an in-depth study of pulsar emission or interstellar medium physics requires observations over wide bandwidths and over different time scales (You et al. 2018; Shannon et al. 2016).

An initial value of a pulsar flux density can be determined from the known survey sensitivity and the S/N of the detected profile. Such flux density estimates have been published by, e.g., Manchester et al. (2001) and, more recently, Stovall et al. (2014). After a pulsar has been discovered, it is normally observed multiple times over at least 1 yr. During this time more accurate flux density determinations can be produced (usually based on comparing the signal strength of the pulsar with that of a pulsed calibration source). Pulsar data sets obtained with the Parkes radio telescope are usually placed on a flux density scale using observations of Hydra A (also known as 3C 218 and PKS 0915−11). This process assumes that Hydra A has a flux density of 43.1 Jy at 1400 MHz and a spectral index of −0.91 over the observation frequency range (Baars et al. 1977). Observations are carried out by pointing directly at Hydra A and also recording data 1 degree offset to the North and South. During each observation, the calibration signal is switched at 11.123 Hz and these observations enable us to scale the measurement of the switched calibration signal with a specific backend instrument to flux density units. We then assume that the flux calibrator is stable between such measurements.

Such calibration observations have been performed over many years (with a cadence of approximately once per month) during Parkes Pulsar Timing Array (PPTA, Manchester et al. 2013) observations. The data were processed and then made available for other observing projects. In particular, numerous results from the PPTA have been combined together to give a small number of averaged flux calibration solutions and some of these are available online[1].

In this paper, we:

- Obtain new flux density measurements in the 20 cm observing band for 32 pulsars.
- Compare flux density solutions acquired with Hydra A with those from another calibration source, PKS B0407−658.
- Quantify the effects of radio-frequency interference (RFI), and its standard removal algorithms, on flux density determinations.

2 CHOOSING THE DATA SAMPLE AND DETERMINING THE FLUX DENSITIES

The CSIRO data archive (see, e.g., Hobbs et al. 2011) contains the majority of pulsar observations collected with the Parkes telescope (with the earliest observation in the archive from 1991). After an embargo period of 18 months,

---

[1] *https://doi.org/10.4225/08/5ab2e8014512d*

the data become publicaly available. We have therefore cross-matched the 20 cm observations available in the archive with the pulsars that have no flux density measurements in the ATNF Pulsar Catalogue. We have also managed to obtain a small number of extra observations with the Parkes telescope for a handful of pulsars. In total we were able to procure observations of 56 pulsars for which no flux densities were previously published in the 20 cm band and have successfully acquired flux density values for 32 of these (the remainder were either undetectable or we only achieved a low S/N pulse profile). The pulsars in our sample are all young, solitary pulsars except for PSR J1157−5112, which is in a binary system with a ∼ 3.5 d period and PSR J1757−5322, which is a millisecond pulsar in a binary system with an orbital period of 0.5 d.

All the observations that we processed were obtained at a central frequency close to 1400 MHz. The majority was acquired with the central beam of the Parkes multibeam receiver (Staveley-Smith et al. 1996). A number of backend systems have been employed for recording the data, including the pulsar wide band correlator (WBC), the Parkes Digital Filterbanks (PDFB1, PDFB2, PDFB3 and PDFB4) and the CASPER Parkes Swinburne Recorder (CASPSR). Details on receivers and backends can be found in Manchester et al. (2013). All data were recorded using the PSRFITS data format (Hotan et al. 2004b) with 30 or 60 s sub-integrations.

The data were processed with the PSRCHIVE pulsar signal processing system (Hotan et al. 2004a). For our primary results, we excised data affected by narrow band and impulsive RFI, and removed 5% of the band edges. We applied PAZI to visually inspect the pulse profiles and to remove frequency channels or sub-integrations affected by RFI. We then employed specific Hydra A flux calibration solutions corresponding to the receiver and backend instrument used. The majority of the calibration solutions was obtained from the data archive. However, we reprocessed all the PPTA observations of Hydra A acquired with the multibeam receiver and PDFB4 backend system. We produced spot-measurements of the calibration solution and also generated a weighted-average of these calibration solutions, providing an averaged solution for this receiver and backend system.

The pulsar observations were calibrated with their associated calibration files using the PSRCHIVE program PAC to flatten the bandpass, transform the polarization products to Stokes parameters and to calibrate the pulse profiles in flux density units. We formed analytic templates from our observations by employing PAAS and then calculated the

flux density estimate using PSRFLUX, which first matches the template with the observation and then determines the area under the template. This is carried out by computing a simple least squares fit in which the measured profile is assumed to be a scaled version of the template with an offset (Demorest, private communication). The uncertainty comes from the least squares uncertainty determination assuming that the reduced χ^2-value of the fit is unity. Of course, this procedure assumes that the template is a good representation of the pulse profile (we discuss below whether this is a reasonable assumption or not). The observations of pulsars for which we have multiple observations were first processed independently, but then combined utilising PSRADD and the flux density procedure was repeated to form a single, averaged flux density value.

For comparison, we also produced data files without any RFI-flagging and files with the automatic PAZ flagging, but without the manual RFI removal. We also computed, for each of our data files, flux density estimates using non-averaged Hydra A flux calibration solutions and, in addition, flux calibration solutions that we derived from observations of PKS B0407−658 (assuming a flux density of 16.02 Jy at 1400 MHz; Kuehr et al. 1981). We also trialled other procedures to measure the flux density of each pulsar, including simply calculating the area under each profile without any assumption about the profile shape.

3 RESULTS AND DISCUSSION

Our primary results are listed in Table 1. In column order we give each pulsar an identification number and then list the pulsar name, pulse period, dispersion measure, observation length, S/N of the pulse profile and the measured flux density obtained using the most up-to-date Hydra A calibration solution. We recommend that these flux density values be included in the next version of the pulsar catalogue. In general, our results are not surprising. Johnston & Kerr (2018) published flux densities for about 600 pulsars at 1.4 GHz with Parkes archive data. Most pulsars in their paper have multiple observations and they add all the data together and present a single flux density for a given pulsar. In order to compare the results from our pipeline with theirs for a given observation, we choose two pulsars (PSRs J0540−7125 and J0758−1528; a weak and a moderately-weak pulsar) with only one observation. We find the flux densities generated by our pipeline are consistent with theirs at a level of 0.1 mJy. The differences could be caused by the various factors we discuss later in this section. We note a strong correlation between the profile S/N and the flux density, and a strong inverse correlation between the profile S/N and the fractional size of the un-

certainty. For the remainder of this paper, we wish to determine how confident we can be in these flux density values and their uncertainties.

3.1 The Hydra A Calibration Solutions

Our flux density values rely on the assumed flux density (and its spectral index) for the radio galaxy Hydra A. The flux density and spectral index at 1400 MHz for Hydra A have been published by different authors (Baars et al. 1977; Kuehr et al. 1981; Lane et al. 2004) and range from ∼43 to 45 Jy. The discrepancies in these published measurements, could, as noted by Jankowski et al. (2018), be caused by different pointing positions along the two radio lobes and are much larger than the formal uncertainties on most of our flux density values. The ratio of these values is 0.96, implying an uncertain scaling factor in any measured flux density value for this factor.

We can also compare our results to those obtained using PKS B0407−658 as the primary calibrator. Over a narrow bandwidth, changing the primary calibrator should simply scale the resulting flux density values by a small factor and we find that our nominal results, listed in Table 1, scale by a mean factor of 0.914 (with a standard deviation of 0.001) when we make use of PKS B0407−658 (i.e., the flux density values are slightly smaller when we use PKS B0407−658 than when we use Hydra A). As we have no prior reason to believe one flux calibrator over the other, we must assume that there is an uncertainty in our measurements of around this factor caused by the choice of flux calibration solution.

We can also trial different flux calibrator solutions derived from different observations of Hydra A. We have chosen to study PSR J1414−6802 for which we have a recent observation and a measured flux density in Table 1 of 0.66(3) mJy. We trialled 168 different Hydra A calibration solutions measured over the last decade. All of these Hydra A calibration observations were carried out using the central beam of the multibeam receiver and PDFB4 backend at a central frequency of 1369 MHz with 256 MHz bandwidth.

Our results are shown in Figure 1 as a function of the time since the Hydra A calibration observation was made. There is a variation in the measured flux density between different calibration solutions. The standard deviation of the flux density values is 0.0094 mJy, suggesting that a single flux density solution will only provide a flux density with a precision of ∼0.01 mJy[2] (a detailed descrip-

---

[2] Note that there is no evidence for any correlation between the measured flux density and the pointing position of the telescope during the flux calibration method.

Table 1 Pulsar Observational Parameters

Psr #	PSR J	Period (s)	DM (cm^{-3} pc)	Length (min)	S/N	Flux density (mJy)
1	J0133−6957	0.46	22.9	14.0	34.5	0.361(12)
2	J0455−6951	0.32	94.9	77.0	11.1	0.083(4)
3	J1006−6311	0.84	196.0	30.0	13.7	0.119(11)
4	J1012−2337	2.52	22.5	15.0	8.2	0.135(13)
5	J1057−4754	0.63	60.0	5.0	7.3	0.53(3)
6	J1157−5112	0.04	39.7	40.0	22.5	0.276(16)
7	J1232−4742	1.87	26.0	5.0	43.6	2.38(6)
8	J1312−5402	0.73	133.0	6.0	29.8	0.78(3)
9	J1312−5516	0.85	134.1	3.5	119.4	3.04(3)
10	J1328−4921	1.48	118.0	6.0	26.3	0.82(3)
11	J1335−3642	0.40	41.7	6.5	4.9	0.27(4)
12	J1350−5115	0.30	90.4	2.5	51.0	1.27(3)
13	J1355−5153	0.64	112.1	17.5	106.5	0.855(9)
14	J1358−2533	0.91	31.3	3.0	4.9	0.15(5)
15	J1414−6802	4.63	153.5	5.9	28.4	0.65(3)
16	J1420−5416	0.94	129.6	3.0	28.5	0.79(3)
17	J1423−6953	0.33	124.0	15.0	24.2	0.362(9)
18	J1457−5122	1.75	37.0	20.0	102.0	1.382(16)
19	J1506−5158	0.84	61.0	2.0	60.4	3.75(8)
20	J1603−2531	0.28	53.8	3.5	196.3	4.98(3)
21	J1610−1322	1.02	49.1	30.0	56.6	1.11(3)
22	J1659−1305	0.64	60.4	30.0	47.2	0.803(17)
23	J1708−7539	1.19	37.0	30.0	52.6	0.747(13)
24	J1711−5350	0.90	106.1	6.0	39.9	0.836(19)
25	J1728−0007	0.39	41.1	30.0	46.0	0.655(15)
26	J1734−0212	0.84	65.0	40.0	26.6	0.279(12)
27	J1749−5605	1.33	58.0	5.5	22.7	0.635(15)
28	J1757−5322	0.01	30.8	20.0	37.3	1.17(4)
29	J1833−6023	1.89	35.0	29.9	123.1	1.459(12)
30	J1857−1027	3.69	108.9	28.3	164.1	2.032(17)
31	J1900−7951	1.28	39.0	27.9	77.4	0.946(12)
32	J2155−5641	1.37	14.0	39.9	31.4	0.361(12)

Notes: In column order, we list pulsar identification number, pulsar name, pulse period, dispersion measure (DM), observation length, S/N for the folded profile and flux densities for the pulsars in our sample. 1σ uncertainties on the last quoted digit are given in parentheses.

tion of the flux density measurements and correlations with changes in the observing system will be described in the forthcoming PPTA second data release publication).

3.2 Measuring the Flux Densities

The flux density values are, of course, dependent upon the method used to make the measurement. Published flux density values represent the signal strength that would be recorded for a point continuum source at the position of the pulsar (i.e., it is determined across both the on- and off-pulse emission). This implies that an estimate of the flux density can simply be made by summing the calibrated pulse profile across all the pulse phase bins (assuming that a baseline has been removed from the off-pulse emission).

In Figure 2 we plot the difference between the flux density calculated by summing the profile bins minus our nominal flux densities (the error bars are taken as uncertainties on the values in Table 1). Simply summing under the profile will be biased high because of the presence of RFI and, for most of the pulsars, we note higher values of ~ 0.05 mJy on average. However, the procedure that makes use of a pulse profile will be affected by any non-
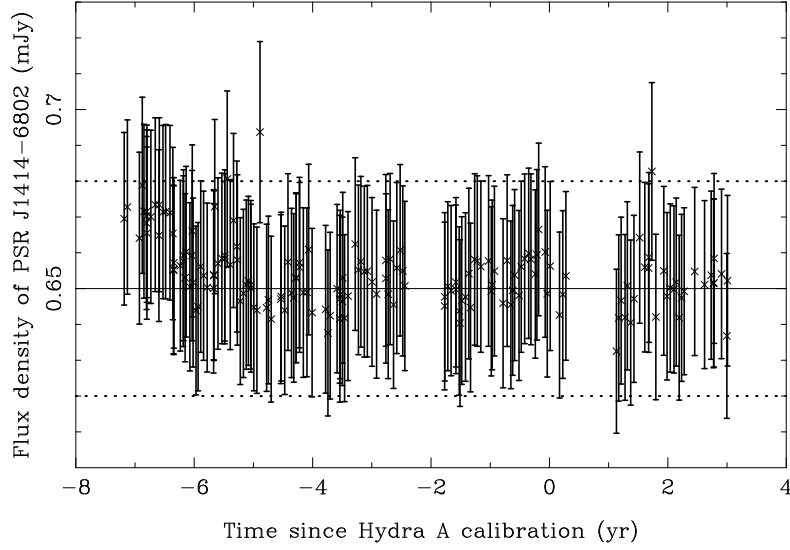
Fig. 1 The flux density of PSR J1414−6802 when determined using different Hydra A calibration solutions. The *solid horizontal line* and the *dotted lines* indicate the flux density of this pulsar as reported in Table 1.
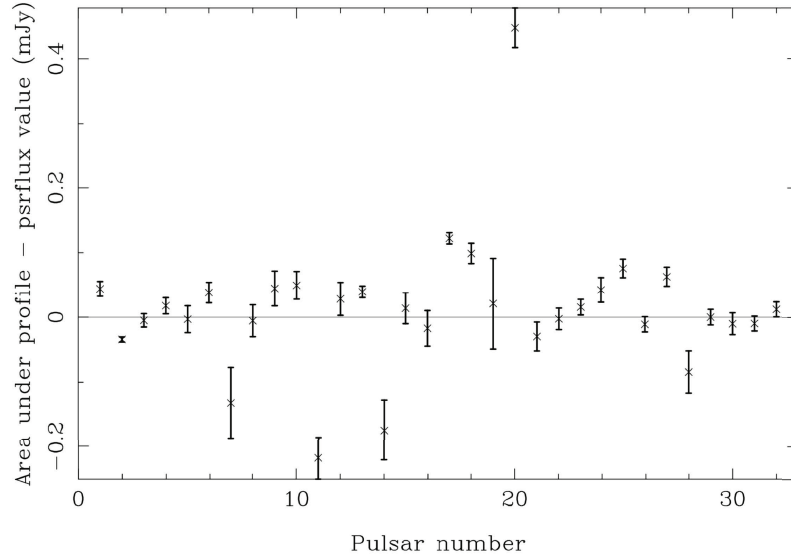

Fig. 2 The flux density measured for each pulsar by simply summing under the profile (with a baseline removed) versus the determination using an analytic pulse template.

perfect match between the analytic template and the actual profile. As small-scale, narrow features are hard to model using existing software, the template procedure is liable to be biased low. Our sample of pulsars PSRs J1457−5122, J1749−5605 and J1857−1027 has two clear components in the pulse profile. For these pulsars, we have created two standard templates. One has only a single component, whereas the other has two or more components. The measured flux densities have, as expected, significantly smaller uncertainties when the template matches the profile and the measured values change by 0.1, −0.25 and 0.1 mJy respectively for the three pulsars.

3.3 Removing RFI

All the methods described above will be affected by RFI present in the profile. However, manual RFI removal is time intensive, difficult to reproduce at a later date and is challenging as we move into the era of very large data sets. We have, therefore, compared how our flux density measurements vary between the nominal results (listed in Table 1), which had both automatic and manual RFI zapping, with profiles obtained with (1) no RFI removal at all and (2) only automated RFI removal (in which the PSRCHIVE package PAZ is applied, with default parameters, to remove frequency channels containing significant
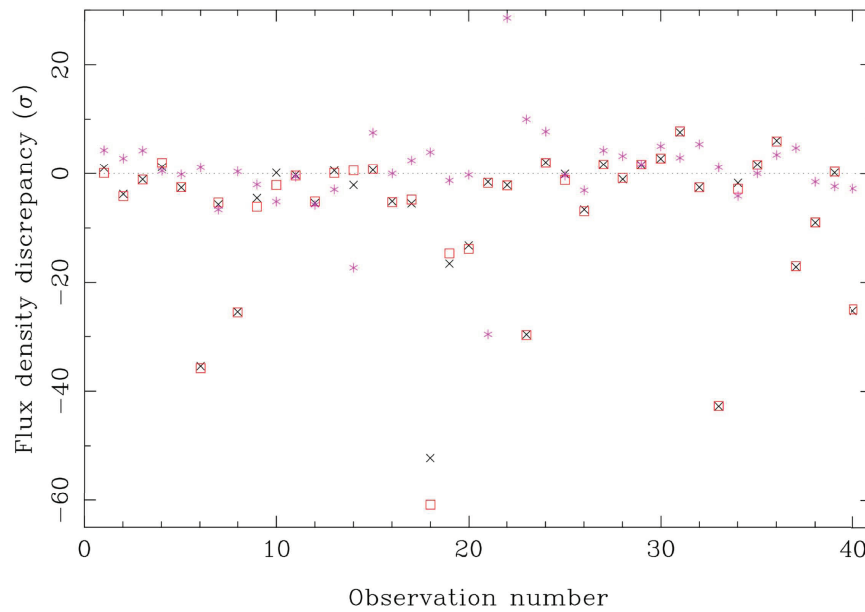
Fig. 3 A comparison between the flux density measurements without any RFI removal (*red squares*) and with a basic, automated scheme (*black crosses*) compared with those from manual RFI zapping. The *purple points* indicate the difference in the measured flux densities when two different people carry out their own manual RFI removal (*Color version is online*).

RFI with a median-zapping routine). Our results are provided in Figure 3. We note that the flux densities measured without manual RFI flagging are usually larger (because the presence of RFI will positively bias the results)[3] and that the flux densities can vary by much more than the uncertainties in the flux density measurements. The differences between no RFI flagging at all and a simple automated method are slight.

Any manual RFI removal will depend on the person doing the zapping. Therefore, we also compare the results provided in Table 1 with the same measurements made by a different co-author on our paper (note that this involves variations in the manual RFI flagging and in the manual determination of the pulse template). In Figure 3, we compare the results given in Table 1 with those determined independently. The root-mean-square deviation is 0.11 mJy. We conclude that current procedures that require no human interaction, and are therefore reproducible and quick, lead to significant variations in the measured flux density values. However, we also note that different individuals carrying out manual RFI flagging procedures will also lead to variations in the measured flux densities.

3.4 Spectral Indices

We combine our flux density measurements with published values reported in different observing bands (close to 300, 600, 700 and 3000 MHz). These are listed in Table 2 as S300, S600, S700 and S3000, respectively. The S1400 column lists our measurement at 1400 MHz. We can use these multi-frequency observations to estimate each pulsar's spectral index, α, assuming a simple scaling law $S_\nu = bx^\alpha$, where S_ν is estimated total flux for a given frequency, ν. Values of b and α are provided in the table. Most of these spectral indices are steeper than the mean values from Jankowski et al. (2018), but our measurements are not particularly unusual as many other pulsars also have similar spectral indices. We do not believe that our pulsar sample is particularly biased towards steep spectrum pulsars and, therefore, this result is simply because of our relatively small sample.

4 CONCLUSIONS

In this paper, we have presented the flux densities at 1.4 GHz for 32 pulsars using the Parkes radio telescope. We have shown that the procedure used in processing the data and calculating the flux densities will affect the final result, usually at a level greater than the formal uncertainties published.

In summary:

---

[3] In a few cases, the flux densities are smaller without manual RFI flagging. This is because some of the actual pulsed signal was removed during the flagging process.

Table 2 Flux Densities and Spectral Indices for Nine Pulsars

PSR J	S300 (mJy)	S600 (mJy)	S700 (mJy)	S1400 (mJy)	S3000 (mJy)	b	α
J1012−2337		1.3		0.135(13)		0.17	−2.66
J1312−5402	41(1)		5(1)	0.78(3)	0.13(4)	1.06(2)	−2.49(1)
J1312−5516		17	12(3)	3.04(3)	0.6(2)	3.39(20)	−2.07(82)
J1355−5153	50(5)			0.855(9)		1.05	−2.63
J1610−1322		7(1)		1.11(3)		1.30	−2.17
J1659−1305		3.2(3)		0.803(17)		0.91	−1.63
J1711−5350			4(1)	0.836(20)	0.19(6)	1.01(33)	−2.22(54)
J1728−0007		4.1(6)		0.655(15)		0.77	−2.16
J1900−7951		5	4(2)	0.946(12)		1.21(21)	−1.86(24)

- Published flux densities for Hydra A, which is commonly applied as the primary flux calibration, vary by a factor of 0.96 at 1.4 GHz.
- Different measurements of Hydra A lead to random variations in the measured flux density values of ∼ 0.01 mJy.
- Using PKS B0407−658 as the primary flux calibrator instead of Hydra A scales the flux density values by a factor of 0.91.
- Various methods to measure a pulsar's flux density from its profile have been proposed. The differing methods lead to changes in the measured flux densities of ∼ 0.05 mJy, which, in some cases, are larger than the formal measurement uncertainty.
- RFI removal schemes can have a large effect on the resulting flux density values (leading to variations of many mJy).

The largest factor in flux density estimation relates to RFI removal. With the existing systems at Parkes, and with the use of Hydra A as the primary flux density calibrator, it is unlikely that a given flux density measurement will be more precise than ∼0.01 mJy.

A spot measurement of a pulsar spectral index has limited applicability as pulsar flux densities vary because of diffractive and refractive scintillation (as well as intrinsic flux variations), but with straightforward calibration schemes it is possible to obtain flux calibrated data sets over many epochs. We will continue this work in the future using both the Parkes and FAST telescopes and we note that there is a large number of pulsars in the catalogue for which we still do not have such basic information as the flux density in the 20 cm band. For instance, there are 49 pulsars detected in early Parkes telescope surveys with no measured flux density measurements and a further four discovered by the Molonglo Observatory Synthesis Telescope. The new Ultra Wideband receiver on Parkes will be ideal for this type of analysis as it is highly sensitive and covers a wide observing band. However, the pulsar catalogue will need to be updated as, currently for each pulsar, a single flux density measurement is recorded in well-defined observing bands. As pulsar flux densities vary in time and frequency, we recommend that the catalogue be updated to store both time and frequency information for each flux density measurement for each pulsar.

The PPTA project will continue to produce flux density calibration solutions for the general user community. The choice of Hydra A is not ideal, in part because the source has extended structure and is not carefully monitored by any observatory. An ideal calibrator would be a bright point source, which has constant flux, and is located in an empty sky field; however, such a target is unrealistic. Unresolved, extragalactic sources typically have stable fluxes (with the notable exception of quasars) and variations in flux densities between observatories can often be attributed to the varying number of external sources in the field. Using an interferometer in conjunction with single-dish observations of a flux calibrator can help to alleviate any discrepancies by sampling with a smaller synthesis beam and imaging potentially complex fields. One such potential flux calibrator candidate is PKS 2251+158 (3C 454.3), which is located at a declination accessible to almost all radio observatories (including both FAST and Parkes).

Calibrating radio astronomy data sets is both essential and non-trivial. With complex telescope systems (such as FAST, in which the surface of the dish and the focus cabin position continuously move during a tracking observation), new ultra-wide-band, or wide field-of-view, receivers and new calibration procedures are becoming necessary. Novel calibration methods such as switching calibration signals at extremely high rates (Li, private communication), injecting pseudo-random-noise sequences, or short duration pulses (Patra et al. 2017) are all currently being explored and we look forward to comparing these methods with the traditional calibration procedures in the near future.

References

Baars, J. W. M., Genzel, R., Pauliny-Toth, I. I. K., & Witzel, A. 1977, A&A, 61, 99

Hobbs, G., Miller, D., Manchester, R. N., et al. 2011, PASA, 28, 202

Hotan, A. W., Bailes, M., & Ord, S. M. 2004a, MNRAS, 355, 941

Hotan, A. W., van Straten, W., & Manchester, R. N. 2004b, PASA, 21, 302

Jankowski, F., van Straten, W., Keane, E. F., et al. 2018, MNRAS, 473, 4436

Johnston, S., & Kerr, M. 2018, MNRAS, 474, 4629

Keith, M. J., Coles, W., Shannon, R. M., et al. 2013, MNRAS, 429, 2161

Kerr, M., Coles, W. A., Ward, C. A., et al. 2018, MNRAS, 474, 4637

Kijak, J., Basu, R., Lewandowski, W., Rożko, K., & Dembska, M. 2017, ApJ, 840, 108

Kuehr, H., Witzel, A., Pauliny-Toth, I. I. K., & Nauber, U. 1981, A&AS, 45, 367

Lane, W. M., Clarke, T. E., Taylor, G. B., Perley, R. A., & Kassim, N. E. 2004, AJ, 127, 48

Levin, L., McLaughlin, M. A., Jones, G., et al. 2016, ApJ, 818, 166

Manchester, R. N., Hobbs, G. B., Teoh, A., & Hobbs, M. 2005, VizieR Online Data Catalog, 7245

Manchester, R. N., Lyne, A. G., Camilo, F., et al. 2001, MNRAS, 328, 17

Manchester, R. N., Hobbs, G., Bailes, M., et al. 2013, PASA, 30, 017

Patra, A., Bates, J. E., Sun, J., & Perdew, J. P. 2017, Proceedings of the National Academy of Science, 114, E9188

Shannon, R. M., Lentati, L. T., Kerr, M., et al. 2016, ApJ, 828, L1

Staveley-Smith, L., Wilson, W. E., Bird, T. S., et al. 1996, PASA, 13, 243

Stovall, K., Lynch, R. S., Ransom, S. M., et al. 2014, ApJ, 791, 67

You, X. P., Manchester, R. N., Coles, W. A., Hobbs, G. B., & Shannon, R. 2018, ApJ, 867, 22